Geofísica Internacional (2025) **64-1**: 1395 - 1415

Investigation of the geothermal system in region of Selime (Turkey) by resistivity methods

Tekin Yeken[1], Nihan Hoşkan[2], Ernam Öztürk[3] and Tahir Serkan Irmak[4]

Abstract

The Anatolian platform continues its development with highly complex tectonic activities in Central Anatolia, known as tectonic deformation. In addition to faulting due to the plate movements, the fluid dynamics in the underground and the thermal cycle are also affected. Heater mass circulation plays a role in the development of plate tectonics. This study was aimed to determine the geothermal potential of Selime (Aksaray) and its surroundings. The resistivity method was applied in field studies for the objectives. Geothermal fields with high thermal potential have been investigated by Vertical Electric Sounding (VES) profiles. In the field study, five vertical electric soundings (VES) were applied, a general resistance of (50 – 60) Ωm was observed, and Selim tuff was determined at a depth of approximately (30-35) m. A sudden resistance drop of (1-2) Ωm under the Selime tuff layer proved the existence of a geothermal source. When examined with the hydrogeological data, a thermal fluid is present with an impermeable cover layer. As a result of this research, it was observed that the heater mass affected the thermal fluid, indicating that circulation represented a shallow system.

Key words: Selime, resistivity, geothermal fluid, heater mass convection.

Resumen

La plataforma de Anatolia continúa su desarrollo con actividades tectónicas de alta complejidad en Anatolia Central, conocida como deformación tectónica. Además de las fallas debidas a los movimientos de las placas, también se ven afectados la dinámica de fluidos en el subsuelo y el ciclo térmico. La circulación de masa calentadora juega un papel en el desarrollo de la tectónica de placas. Este estudio tuvo como objetivo determinar el potencial geotérmico de Selime (Aksaray) y sus alrededores. Se aplicó el método de resistividad en estudios de campo para los objetivos. Los campos geotérmicos con alto potencial térmico han sido investigados mediante perfiles de Sondeo Eléctrico Vertical (VES). En el estudio de campo se aplicaron cinco sondeos eléctricos verticales (VES), se observó una resistencia general de (50 – 60) Ωm y se determinó la toba Selim a una profundidad de aproximadamente (30-35) m. Una caída repentina de resistencia de (1-2) Ωm debajo de la capa de toba de Selime demostró la existencia de una fuente geotérmica. Cuando se examina con los datos hidrogeológicos, se encuentra presente un fluido térmico con una capa de cubierta impermeable. Como resultado de esta investigación se observó que la masa calentadora afectaba al fluido térmico, indicando que la circulación representaba un sistema poco profundo.

Palabras clave: Selime, resistividad, fluido geotérmico, convección de masa calentadora.

Received: September 8, 2023; Accepted: November 7, 2024; Published on-line: January 1, 2025.

Editorial responsibility: Dr. Jorge Alejandro Wong Loya

* Corresponding author: Ernam Öztürk, er77turk@gmail.com.
[1] Kocaeli University, Hereke Asım Kocabıyık Vocational School, Kocaeli, Turkey.
[2] İstanbul University, Cerrahpaşa Faculty of Engineering-Department of Geophysics, İstanbul, Turkey.
[3] Düzce University, Construction Department, Düzce, Turkey.
[4] Kocaeli University, Faculty of Engineering-Department of Geophysics, Kocaeli, Turkey.

Tekin Yeken, Nihan Hoşkan, Ernam Öztürk, Tahir Serkan Irmak

https://doi.org/10.22201/igeof.2954436xe.2025.64.1.1738

1. Introduction

Hydrothermal systems, one of the most common types of geothermal reservoirs, are frequently made up of three fundamental features: a heat source, groundwater transport, and a confining impermeable layer (i.e. clay cap) (Pellerin *et al.* 1996; Cumming 2009; Munoz 2014; Samrock *et al.* 2015; Tank and Karaş 2020) If the porosity and permeability of the host rock and top soil layers allows, the heated fluids can raise to the near-surface forming diverse geothermal surface features such as steaming grounds, fumaroles, hot springs, geysers, mud pools and collapse craters (Lloyd 1959; Hedenquist and Browne 1989; Montanaro *et al.* 2023; Gomez *et al.* 2023).

Turkey has a huge geothermal potential and heat flux, due to young volcanism and magmatism (Çetin *et al.* 2020). The first geothermal exploration surveys in Turkey were carried out in 1961–1962 by the Directorate of Mineral Research and Exploration (MTA). Studies performed by the General Directorate of Mineral Research and Exploration (MTA) since 1962, have determined 170 geothermal fields in the Aegean region, Northwest Anatolia and Central Anatolia (Benli 2013). The geothermal systems of Turkey were mainly formed in recent and regional structural lines and are more frequently in regions of recent tectonism and Tertiary volcanism and/or metamorphism (Korkmaz *et al.* 2014).

The volcanism in the Central Anatolia is continental arc type (Pasquare *et al.* 1988; Kıyak *et al.* 2015). There is a low velocity upper mantle region beneath this area obtained by seismological studies (Gans *et al.* 2009; Kıyak *et al.* 2015) The extensional crustal stresses particularly in Eastern and Central Anatolia, led to the development of vast volcanic fields between the Miocene and the Holocene. There are several hydrothermal manifestations and some indications of high-heat flow at these volcanic fields (Korkmaz *et al.* 2014).

In a Curie point study of Turkey suggested that the 580 °C isotherm contour around the Cappadocia Volcanic Province (CVP) could be a potential reservoir for a geothermal system (Kıyak *et al.* 2015). Ziga hot springs which locate the geothermal reservoir and a resistive zone due to uprising of basement at the center-around L2900-are the characteristic features of the western part of the investigated area (Ilkişik *et al.* 1997). The low resistivity zone of 5 Ohm m is Selime tuffs. The depth of the resistive (2000-9500 Ohm m) basement, that is interpreted as the Paleozoic Bozqaldag Formation (limestone/marble, gneiss and quartsite, and the thickness of the overlying conductive Selime tuff and Kizilkaya ignimbrites increases eastward (Ilkişik *et al.* 1997).

Generally, the use of geothermal energy in Turkey is based on the production of hot water, hot water places are usually far from housing. Because of having high heat flux and higher undisturbed ground temperature values, shallow geothermal energy potential offers a good choice in terms of heating and cooling buildings (Çetin *et al.* 2020). The geothermal potential and dependency on imported energy sources are stimulating geothermal energy exploration and development projects in Turkey (Serpen *et al.* 2009; Başel *et al.* 2010; Bayrak *et al.* 2011).

The general purpose of the electric and electromagnetic methods of geophysical exploration is to estimate the distribution of the ground electrical resistivity. Such surveys are widely used in ground water applications because of an association between resistivity and subsurface water content (Keller and Frischknecht, 1966; McNeill, 1990; Ward, 1990; Kirsch, 2006; Flores and Moya, 2011).

Gyulai *et al.*, 2016 used 2.5D CGWI combined geoelectric weighted inversion of VES measurements for characterizing geoelectrically the thermal water aquifers. According to their technique, which uses the joint 2D forward modeling of dip and strike direction data, the 3D structures can be determined (Asfahani, 2021).

The geophysics also gains emphasis for being a non-invasive method, applicable to a wide variety of scales showing the possibility of obtaining geological information at great depths, regardless of rock exposures and description of drill cores (Lowrie, 2007; Dentith & Mudge, 2014; Cortes *et al.* 2016).

Geothermal resources can be detected by electromagnetic (EM) and direct conductivity (DC) methods, since they produce strong variations in subsurface electrical resistivity (Berktold 1983; Meju 2002). DC resistivity is a better method for the monitoring of geothermal resources at shallow depths (Bayrak *et al.* 2011). Hydrothermal fluids modify the electrical resistivity based on the fluid content of surrounding geological formations (Kıyak *et al.* 2015). Resistivity is controlled by ionic conduction through fluids in pore spaces, rather than by electronic conduction through the mineral matrix (Ilkişik *et al.* 1997).

This study aims to determine the Selime region's geothermal potential and its surroundings. Selime area has tourism potential at a distance of 5 km to the northwest of the Ihlara Valley. 5 vertical electric drilling (VES) studies were carried out in the field. The findings prove the existence of hot water. A detected geothermal area close to the big city center is advantageous compared to distant regions in using that geothermal area for heating and energy. Selime part is closer to the Aksaray city center than the hot springs in Ihlara Valley and Ziga thermal region.

2. Materials and Methods

The resistivity method is based on measuring the potential distribution of the electric field occurring in the ground. The

method aims to determine the resistivity-conductivity values arising from the physical differences of the rocks. In geothermal reservoir research, it is preferable to determine the boundaries of the vertical and lateral directions of different geological structures as the primary method. In this application, Schlumberger-oriented resistivity method was used for the objective.

3. Geology

Central Anatolia is an orogenic plateau that corresponds to the backarc basin of the Cyprus subduction zone, located between the Pontides to the north and the central Tauride Mountains to the South (Figure 1 – Figure 4a – Figure 7a). The Neotectonic regime in the central Anatolia has been dominantly characterized by compressive and strike-slip fault motions, accompanied by an intense and widespread volcanic activity concentrated within a triangular zone between major oblique fault zones, the Ecemiş and Tuz Gölü fault zones (Figure 7a,b) (Piper *et al.*, 2002; Hacıoğlu *et al.* 2023). The Cappadocian Volcanic Province in central Anatolia represents one of the most prominent examples of arc volcanism associated with continental collision developed as a result of the convergence of the Afro-Arabian and Eurasian plates in eastern Mediterranean since late Miocene times (~ 5 Ma) (Hacıoğlu *et al.* 2023). Volcanic products in the Cappadocian region mostly consist of a set of rhyodacitic and rhyolitic ignimbrites associated with Neogene deposits and Neogene and Quaternary volcanoes (Pasquare *et al.*, 1988; Froger *et al.*, 1998; Hacıoğlu *et al.* 2023). The volcanism in the central Anatolia was accepted to develop in the tectonic depressions by Pasquare *et al.* (1988). CVC starting from Aksaray to Kayseri is totally covered by Neogene ignimbrites and, lava-ash flows and tuffs of Mt. Melendiz and Mt. Hasan. The initial volcanic activity was probably started in the mid to Upper Miocene (Besang *et al.*, 1977) by the andesitic gray-coloured lava flows (Kecikalesi volcanites) (Koşaroğlu *et al.* 2016) (Figure 1). The study area mainly consists of Bozçaldağ metamorphics consisting of paleozoic marble, gneiss, and quartzites. The lower Pliocene Göstük ignimbrites overlie Bozçaldağ metamorphics, and the Göksük ignimbrites overlie the Uzunkaya formation unconformably. This Lower Pliocene formation comprises volcanic material, tuff, conglomerate, sandstone, claystone, and limestone (Öktü and Kalkan 1984). It is observed that the Uzunkaya formation, which is represented by the alternation of sandstone, is transitive with Lower Pliocene Kızılkaya ignimbrites. These units follow the Selime tuff and red colored Kızılkaya ignimbrite of the same aged tuffs. Kızılkaya ignimbrites originated after the wear phase of the Selime tuffs, covering the Selime tuffs with the Uzunkaya formation as discordant. (Figure 3 – Figure 2). The precipitation of $CaCO_3$ forms travertines due to CO_2 of Ca(HCO)3 contained in deep waters coming from the surface. Travertine is widely observed in Yaprakhisar, Selime, and the surrounding area. In addition to the west of Acigöl and the village of Selime, there are travertine outcrops. Travertines have a whitish-yellowish porous and perforated structure, and their thickness varies between 1-30 m. Kızılkaya ignimbrite (Tk) is white, dirty white, and light pink. It is seen as a column structure due to the cooling cracks developed in the vertical direction, (Figure 3 – Figure 2). Karakaya Formation is one of the most common geological units in the research area. It is observed near the village of Selime (Figure 4). This formation consists of various volcanic compositions such as tuff, tuffite, sandstone, conglomerate, and claystone. It is yellowish, greenish, and brown. Selime tuff (ts), a very common geologic formation in the study area, is known for its yellowish-white-light pink colors (Beekman 1966; Öktü and Kalkan 1984). Selime tuff (ts), which is usually a product of acidic volcanism, is highly resistant to abrasion. This unit represents a typical and massive approximately 60-100 m in thickness around Selime and Yaprakhisar region. Tuffs are also observed in the northeast of Kızılkaya ignimbrite (Figure 2 – Figure 3). In addition, Selime Tuff (ts) is seen under the Kızılkaya ignimbrite in the south of Ihlara Valley, located from Yaprakhisar to Belisırma. In many parts of the research area, the Kızılkaya ignimbrites covered the Selime tuffs, thereby prevented the abrasion of the Selime tuff (ts). The geothermal systems of Turkey were mainly formed in recent and regional structural lines and are more frequently in regions of recent tectonism and Tertiary volcanism and/or metamorphism (Korkmaz *et al.* 2014). Although identified geothermal resources in the Ihlara Valley are modest, substantial undiscovered fields have been inferred primarily from the volcanic and tectonic setting but also from the high regional heat flow on the Kırşehir Massif. (Ilkişik *et al.* 1997). There are five main thermal zones along the Ihlara Valley (Figure 2 – Figure 4a), such as: Yaprakhisar, Ziga, Belisırma, Ihlara and Ilısu (Ilkişik *et al.* 1997). The temperatures of the geothermal springs in the region are about 24-51°C (Ilkişik *et al.* 1997). Water temperatures in the study area and its surroundings vary between (40-69) °C (Figure 4c). There are two thermal hotels, one under construction, 2 km away southeast of the study area (Figure 2).

4. Regional Geothermal and Water Characteristic

In 2004, MTA took samples from 13 surface water springs in the Ziga geothermal region and conducted hydrochemical analyses. The analysis results are shown in Table 1. The Waters in the area are Na-Cl type waters with non-carbonate alkalinity

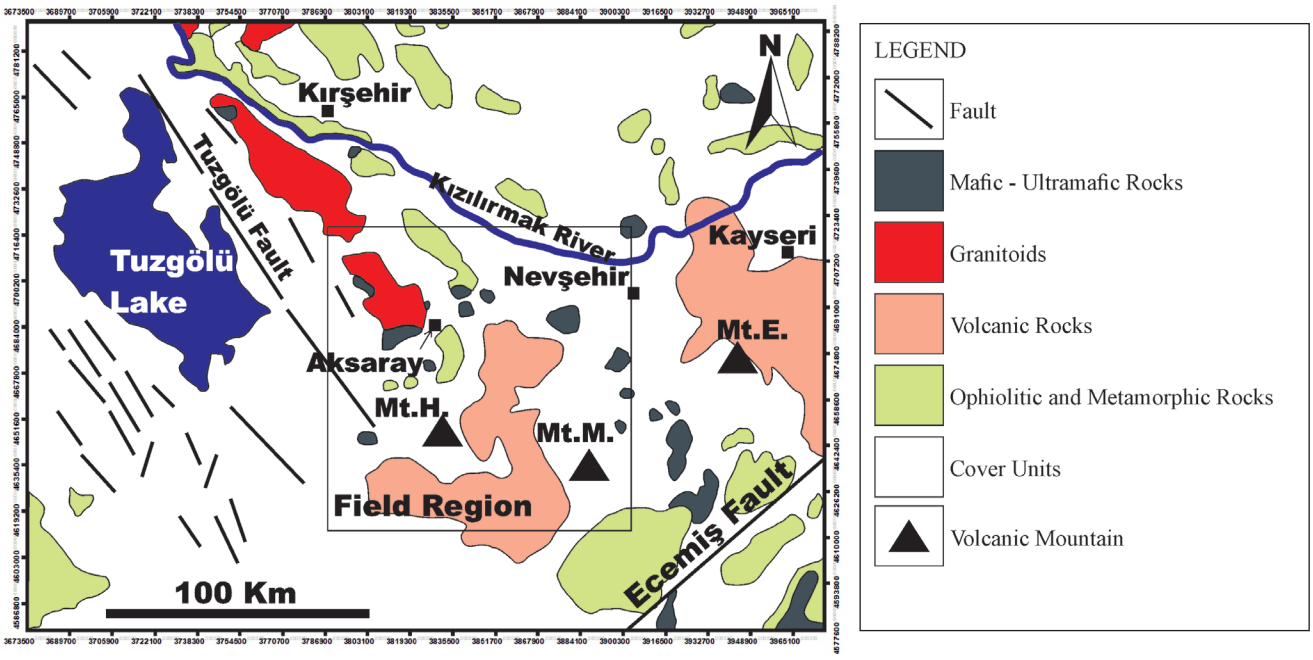

Figure 1. Simplified geological map of Central Anatolian (Ateş *et al.* 2005; Aydemir 2009; Aydemir *et al.* 2019) (Explanations; Mt.H. Mountion Hasan Volcano, Mt. M. Mountion Melendiz Volcano, Mt. E. Mountion Erciyes Volcano).

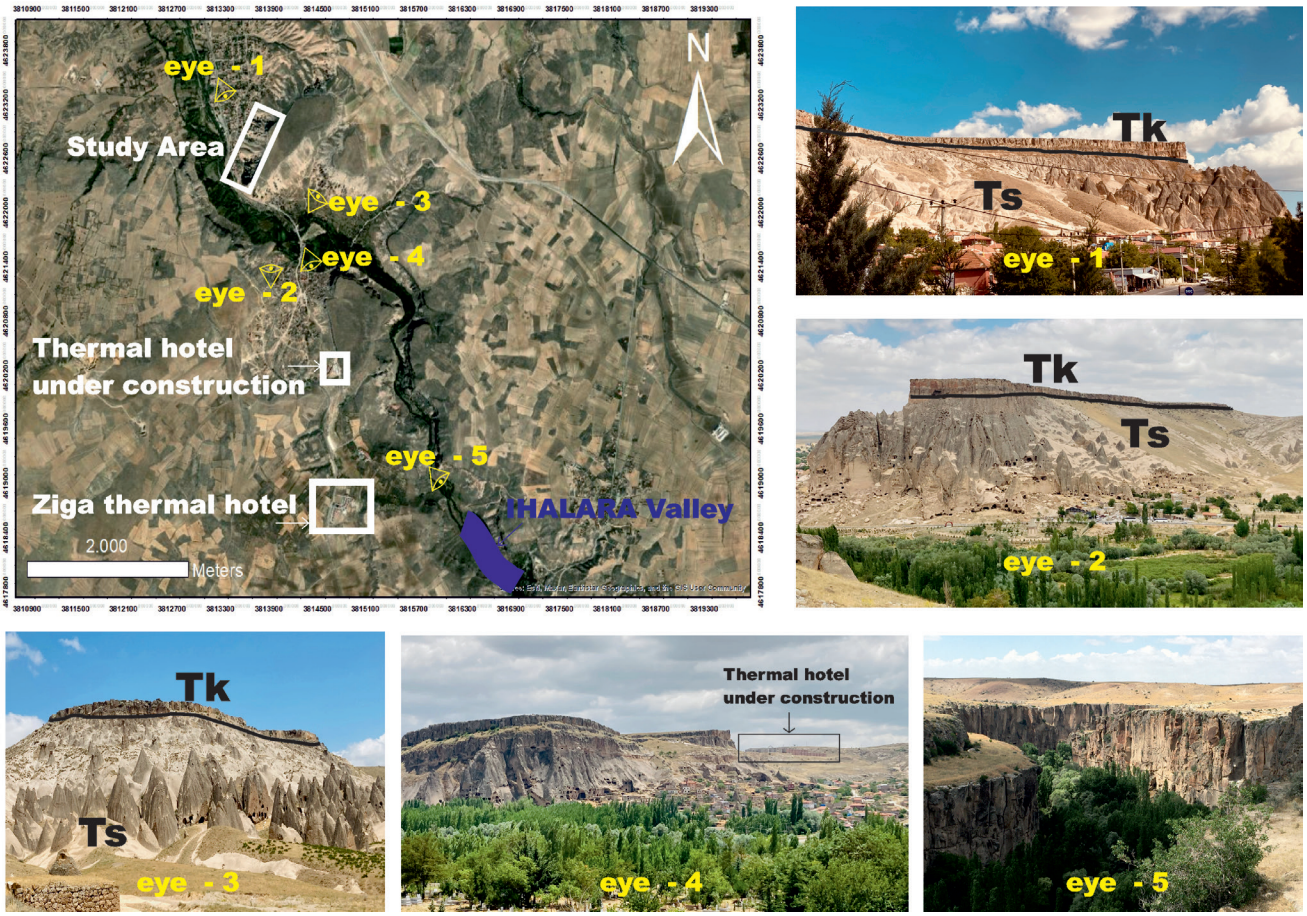

Figure 2. Photos of the study area (Explanations; Selime tuff (Ts) and Kızılkaya ignimbrite (Tk)).

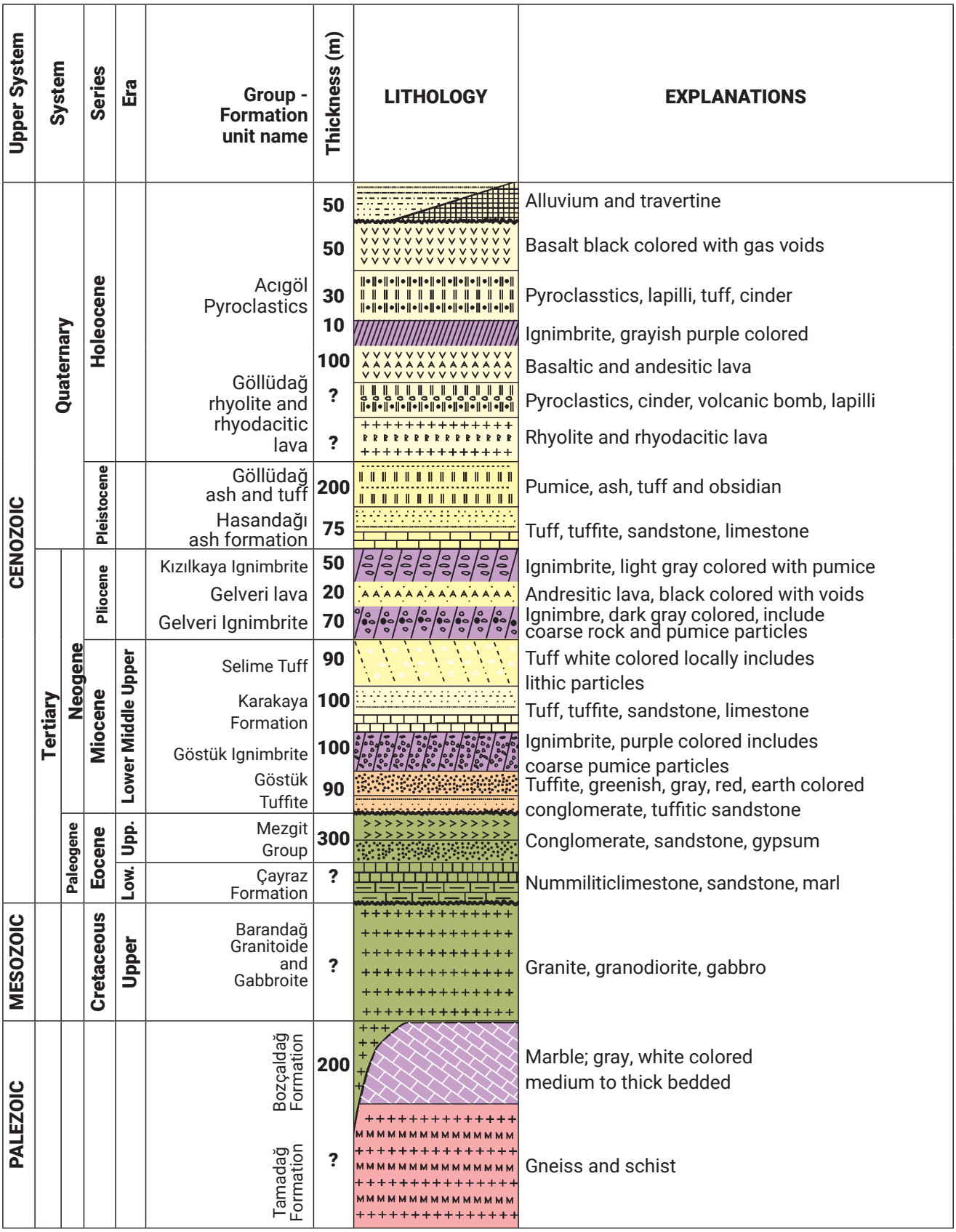

Figure 3. Stratigraphic section of the region (Beekman, 1966, Ayhan and Papak, 1988, Burçak, 2006).

Table 1. Water analysis results of the region (MTA, 2004).

No	Y	X	Z	Temp °C	pH	Ca (mg/L)	Mg (mg/L)	Na (mg/L)	K (mg/L)	Cl (mg/L)	SO_4 (mg/L)	HCO_3 (mg/L)	B (mg/L)	SiO_2 (mg/L)	TDS (mg/L)
M1	610875	4238125	1260	39	6.5	276	46	1175	150	1889	72	1165	32.6	47	4852.6
M2	610850	4238200	1260	37.5	6.5	300	41	1225	156	1907	78	1208	33.4	47	4995.4
M3	610800	4238300	1265	51	6.9	309	49	1160	158	1900	65	1244	32	47	4964
M4	610850	4238225	1255	46	6	300	36	1180	162	1880	71	1208	32.6	75	4944.6
M5	610875	4237575	1190	47.5	6.6	361	39	1212	168	1900	73	1506	29.8	91	5379.8
M6	610891	4238377	1268	50	7.13	270	75.6	946	124	1294	42.6	1722	26	45	4474.2
M7	610908	4238344	1261	44.6	6.62	278	58.4	1088	164	1434	43.9	1739	32	62	4899.3
M8	610017	4238766	1280	32.9	6.53	212	162	830	118	1220	39.9	2087	23	48	4668.9
M9	611769	4237608	1176	43.4	7.07	187	75.8	1161	174	1558	59.6	1797	40	109	5211.87
M10	617681	4232723	1295	35.9	7.47	31.2	49.2	49.2	17.9	20.9	10.1	290	1.7	114	591.67
M11	617703	4232547	1306	29.6	7.42	33.9	10.6	51.1	18.1	30.9	0.96	273	0.9	94	513.46
M12	609883	4238408	1291	16.8	7.66	65.9	19.4	12.7	8.67	7.46	6.73	336	0.7	57	456.86
M13	603616	4244598	1184	14.3	7.8	59.1	12.2	11.7	2.04	7.1	11	244	0.6	52	399.74

greater than carbonate alkalinity, and the waters in samples M10 and M11 are Ca-HCO_3 type waters with carbonate hardness over 50%.

Yaprakhisar Village and its surroundings, located on the border of Ihlara Valley, have been designated as "Ziga Geothermal area".Two hot water wells are located within the Yaprakhisar Village Ziga Thermal Springs (Figure 2 – Figure 4a). The depth of the Ziga-1 well is 250 meters and has a flow rate of 140 l/sec. The depth of the Ziga-2 well is 400 meters and has a flow rate of 120 l/sec. A hydrochemical study was carried out in the Yaprakhisar Ziga region in 2019 by the Turkish Scientific and Technical Research Council (TUBİTAK) in the "Evaluation of Geothermal Resources Project."

Thermal water samples were taken from Ziga-1 and Ziga-2 wells in the Ziga geothermal area within the project's scope in April 2019. (Figure 4 – Figure 2). On-site measurements (pH, EC, temperature, dissolved oxygen, and salinity) were made during the sample collection. The highest Electrical conductivity (EC) value in Aksaray province was measured in the Ziga-1 well (Table 2). A high EC value indicates that the thermal waters have deep circulation. The pH value in Ziga geothermal wells was measured below seven and is acidic. The water temperature was measured as 43.6 °C in the Ziga-1 well and 54.2 °C in the Ziga-2 well.

The central cation in Ziga well water is sodium (Na^+). Next comes calcium (Ca^{2+}) and potassium (K^+). As for anions, chloride (Cl^-) is the highest observed anion in the Ziga-1 well, and

Table 2. Major ion measurement results.

Locations	EC (µS/cm)	pH	T °C	Salt	DO (mg/L)	TDS (mg/L)	Ca (mg/L)
Ziga - 1	6810.00	6.59	43.60	3.66	2.30	3600.00	549.00
Ziga - 2	6720.00	6.64	54.20	3.73	2.60	3610.00	561.00
Locations	Na (mg/L)	K (mg/L)	Mg (mg/L)	HCO_3 (mg/L)	CO_3 (mg/L)	SO_4 (mg/L)	Cl (mg/L)
Ziga - 1	761.00	123.00	47.00	21.54	2.86	75.48	1460.71
Ziga - 2	803.83	128.56	48.53	1590.20	4.31	74.44	1473.09

Table 3. Major ion sequence and water class.

Locations	Cation Sequence	Anion Sequence	Water Class
Ziga - 1	Na>Ca>K>Mg	$Cl>SO_4>HCO_3>CO_3$	Na-Ca-Cl
Ziga - 2	Na>Ca>K>Mg	$HCO_3>Cl>SO_4>CO_3$	Na-Ca-Cl-HCO_3

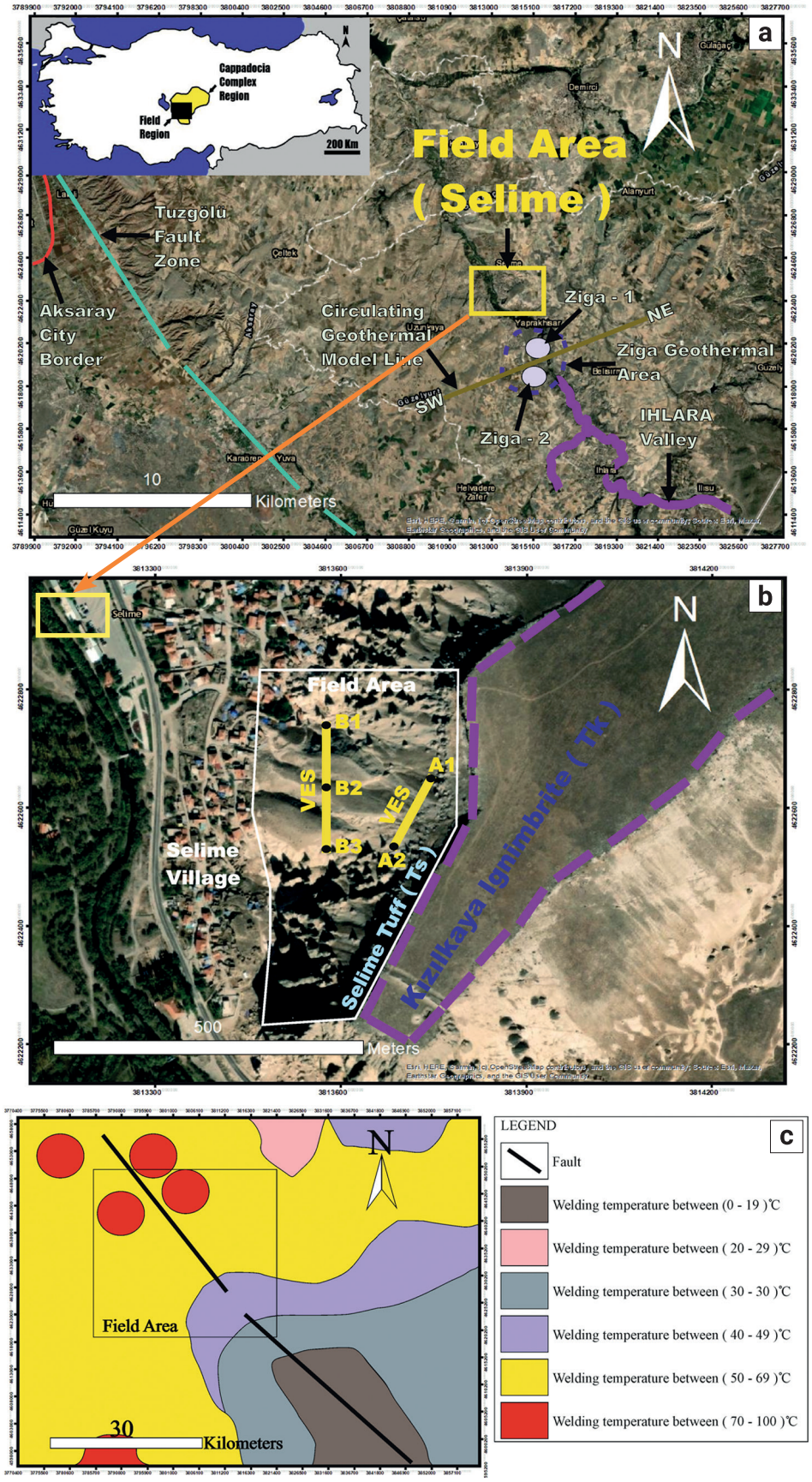

Figure 4. (a) Field Area location and Cappadocia Complex Region (b) Field Study (Selime) and VES (A1,A2 – B1,B2,B3) (c) Simplified geothermal map of Field Study (MTA-Mineral Research and Exploration of Turkey).

bicarbonate (HCO_3^-) is the highest observed anion in the Ziga-2 well (Table 5). It is seen that Ziga-1 and Ziga-2 well waters have similar primary ion contents, as seen in the Schoeller diagram (Figure 5b). The highest Cl content in Aksaray province was measured in the Ziga-2 well. The high Cl content in the Ziga-2 well may be related to the saline units of the Whiting Group rocks rather than the deep-rooted circulation (Burçak 2006; TUBİTAK 2019).

According to the Piper diagram, Ziga thermal waters represent "non-carbonate waters with an alkalinity of more than 50%". The class of thermal water taken from Ziga-1 is Na-Ca-Cl, and the class from Ziga-2 is Na-Ca-Cl-HCO_3. (Figure 5a, Table 3).

Saturation index values of thermal water samples were calculated with the PHREEQC interface of the AquaChem program. With the program, water can be transformed into anhydrite ($CaSO_4$), aragonite ($CaCO_3$), calcite ($CaCO_3$), chalcedony (SiO_2), dolomite ($CaMg(CO_3)_2$), fluorite (CaF_2), gypsum ($CaSO_4 + 2H_2O$), halite (NaCl), quartz (SiO_2) and talc ($3MgO_4SiO_2H_2O$) minerals as discussed. Ziga-1 healthy waters are only saturated with quartz minerals, and other minerals are under saturation. Ziga-2 healthy waters are saturated with aragonite, calcite, dolomite, and quartz minerals. This situation shows that calcite, aragonite, and dolomite crusting can be seen in the carrier systems where the waters of the Ziga-2 well are used. (Table 4).

Table 4. Saturation Index (SI) values

Locations	Anhydrite	Aragonite	Calcite	Chalcedony	Dolomite
Ziga - 1	-1.49	-0.79	-0.66	-0.17	-1.89
Ziga - 2	-1.47	1	1.13	-0.23	1.72
Locations	Fluorite	Gypsum	Halite	Quartz	Talc
Ziga - 1	-0.73	-1.38	-4.68	0.2	-3.21
Ziga - 2	-1.04	-1.44	-4.69	0.1	-1.94

Table 5. Heavy Metals

Locations	As (mg/L)	Br (mg/L)	Cu (mg/L)	Cr (mg/L)	NO_3 (mg/L)
Ziga - 1	1.09	2.05	<0.005	<0.002	<0.27
Ziga - 2	1.09	2.06	<0.005	<0.002	<0.27
Locations	Ni (mg/L)	Mn (mg/L)	Pb (mg/L)	Si (mg/L)	Zn (mg/L)
Ziga - 1	<0.002	0.18	<0.0005	17.76	0.00
Ziga - 2	<0.002	0.18	<0.005	19.31	0.00

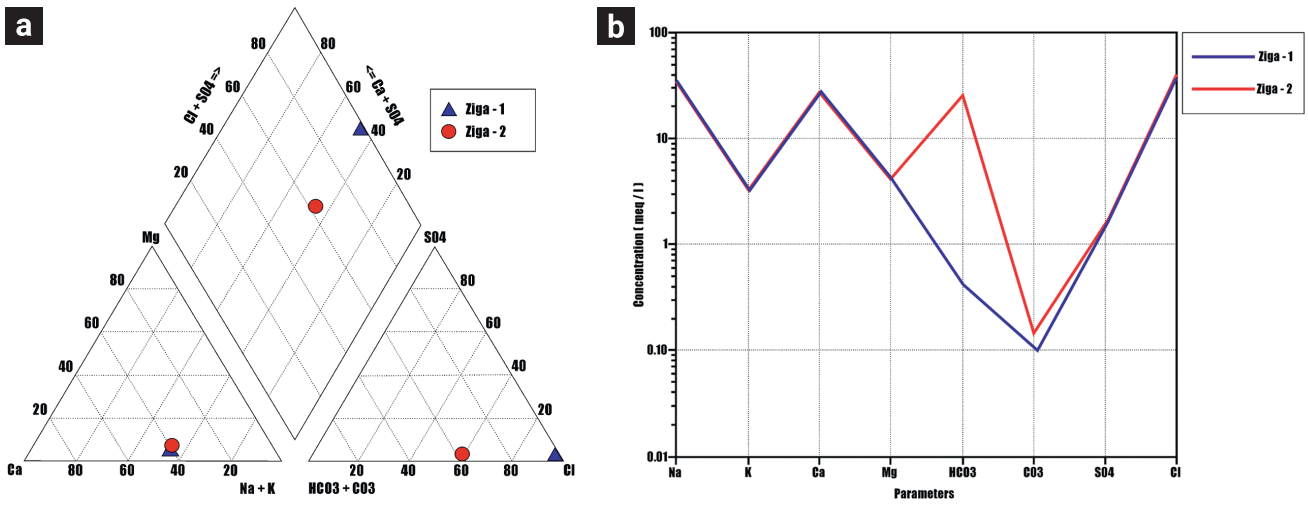

Figure 5. (a) Piper Diagram and (b) Schoeller Diagram.

Within the scope of the project, the As, B, Br, Cr, Cu, Ni, Mn, Pb, Si, Zn and NO3 contents of the waters were analyzed (Table 5). Groundwater absorbs major elements and heavy metals depending on parameters such as rock type, circulation time, temperature, etc. Thermal waters, mainly in thermal springs, are also considered drinking cures.

Geothermometer applications play an essential role in determining reservoir temperatures in geothermal systems. Chemical geothermometers help determine the chemical exchange balance between underground temperature and fluids depending on rock-water interaction. To determine the applicability of geothermometers depending on the chemical structure of hot water, a triangle-shaped diagram was developed by Giggenbach (Giggenbach 1988; TUBİTAK 2019).

This diagram shows geothermometer results quickly, and the validity of cation geothermometer relations can be checked. The diagram briefly consists of three parts: raw waters where the water-rock relationship is not in balance, waters where the water-rock relationship is partially balanced (mixed waters), and waters where the water-rock relationship is in total balance (TUBİTAK 2019).

(Giggenbach, 1988) points out that cation geothermometer results of waters located in the raw water region will not be reliable. According to the cation maturity diagram of Giggenbach (1988), the waters taken from the Ziga geothermal area are located in the "raw waters that have not established water-rock balance" region (Figure 6).

For this reason, cation geothermometers will give incorrect results when calculating reservoir temperatures. Silica geothermometers were used to estimate reservoir temperatures in the Ziga geothermal field. According to chalcedony and quartz geothermometer calculations, reservoir temperatures in the Ziga geothermal field were 58.65 - 106.86 °C (Table 6).

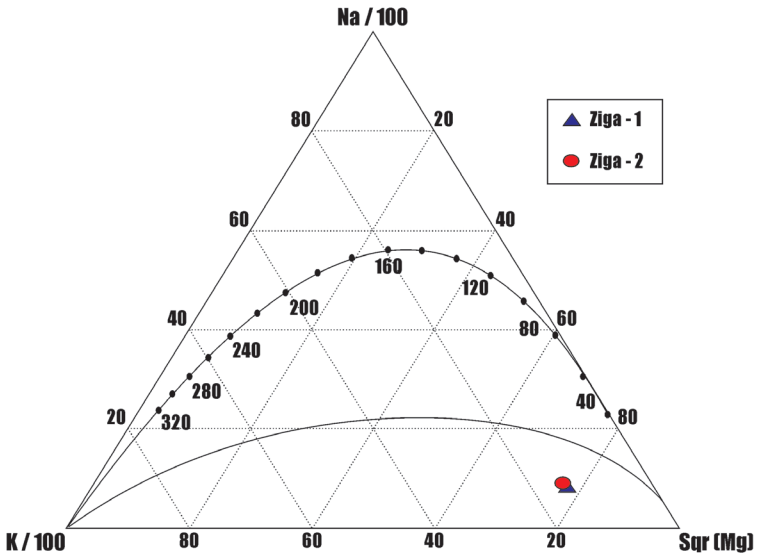

Figure 6. Equilibrium States in the Na-K-Mg Triangle of Ziga Geothermal Fluid.

Table 6. Geothermometer Values Calculated in the Fluid in the Ziga Geothermal Field

Applied Geothermometers		Chamber Temperature °C	
		Ziga - 1	Ziga - 2
SiO_2 (chalcedony)	Fournier, 1977	58.65	62.57
SiO_2 (quartz)	Fournier, 1977	89.42	93.11
SiO_2 (quartz vapor loss)	Fournier, 1977	91.81	95.02
SiO_2 (quartz vapor loss)	Arnorsson *et al.*, 1983	65.7	69.03
SiO_2 (quartz vapor loss)	Arnorsson *et al.*, 1983	90.42	93.65
SiO_2	Fournier, Potter, 1982	99.66	106.86

5. Regional Tectonics

The geodynamic evolution of Turkey is mainly controlled by drift and collision of a number oceanic and continental plates or terranes. This can be ascribed to four orogenic episodes, namely: the Cadomian, Variscan, Cimmerian and Alpine (Göncüoğlu 2019). During these episodes, terranes were formed in a wide range of tectonic settings, including active and passive continental margins, rifts, arcs and suture complexes between the Gondwana supercontinent in the South and the Eurasian supercontinent in the North. (Göncüoğlu 2019).

The classification of the Turkish terranes is mainly based on their configuration, where a number of terranes of continental crust origin were separated by three main oceanic branches of Neotethys (Göncüoğlu 2019).

From South to the North these are: the SE Anatolian Autochthon at the northern edge of the Gondwanan Arabian-Libyan Platform; the SE Anatolian Ophiolite Belt including the remnants of the southern branch of Neotethys; the Tauride-Anatolide Terrane, an Alpine unit of continental crust origin; the Izmir-Ankara-Erzincan Ophiolite Belt, representing the allochthonous oceanic assemblages and subduction-accretion complexes of the Neotethyan Ocean; the Sakarya Composite Terrane, including products of at least two orogenic events; the Intra Pontide Ophiolite Belt, remnants of the northern branch of the Neotethys; the Istanbul-Zonguldak Terrane of continental crust origin and lastly the Istranca Terrane, a suspect terrane of Laurasian affinity (Göncüoğlu 2019).

The Izmir-Ankara-Erzincan Suture Belt (Figure 7a - Figure 8) comprises the remnants of the Neotethyan İzmir-Ankara-Erzincan branch. It consists of different parts of the oceanic lithosphere, together with the subduction-accretion mélanges. Izmir-Ankara-Erzincan that were formed along subduction zones and emplaced southward onto the Tauride-Anatolide Platform during its Late Cretaceous closure.

The suture belt is overthrust by the Sakarya Composite Terrane, characterising the active margin of the Izmir-Ankara-Erzincan Ocean. The ophiolites include dismembered bodies of oceanic lithosphere formed in various tectono-magmatic settings such as the mid-ocean ridges, arcs and supra-subduction-type arc basins as well as intra-plate formations including ocean islands and oceanic plateaus.

The oldest ages obtained yet (Sayit *et al.* 2015) are Carnian whereas the youngest ones from mainly back-arc type basalts are Cenomanian. This suggests that the formation of Izmir-Ankara oceanic crust started as early as Middle Triassic (Figure 7a) and lasted until Late Cretaceous (Tekin *et al.* 2002; Göncüoğlu *et al.* 2015).

As is so far known, along all three oceanic branches of Neotethys oceanic lithosphere generation was vanished by the end of Cretaceous and the Early Tertiary was a period of late orogenic compression, when extensive fore-land and fore-deeptype flysch basins were generated on the passive margins of Istranca, Sakarya, Tauride-Anatolide and SE Anatolian terranes.

The ongoing subduction in corresponding suture zones, on the other hand, mainly produced continental arc-type magmatism in the active margins of these terranes. The collision of continental plates along the northern branch of Neotethys in NE Anatolia has resulted in a change in the geochemistry of the igneous activity from arc-related (Kaygusuz *et al.* 2008) towards post-collisional extension due to break-off of the subducting slab or lithospheric delamination.

The main Paleogene basins in Central Anatolia (e.g. Erzincan, Sivas, Çankırı, Haymana and Tuz Gölü-Ulukışla basins) are formed above the Izmir- Ankara- Erzincan suture belts.

The Neotectonic period, in general, is defined as the study of the post-Miocene structures and structural history of the Earth's crust (AGI 2009). In Turkey, the term covers the Late Miocene-Quaternary time-span and is mainly triggered by the collision of the Anatolian plate and the Arabian promontory.

The convergence ruptured the Anatolian continental crust along the left-lateral East Anatolian Transform Fault (Koçyiğit *et al.* 2001) and the right-lateral North Anatolian Transform Fault that dissects north Anatolia in E-W direction (Şaroğlu *et al.* 1992). Along these main structures the main trunk of Anatolia escaped towards the west (Figure 7a).

The westward extrusion of the Anatolian wedge is accompanied by anticlockwise rotation as well as translation. This is attributed to a response of the continental lithosphere moving laterally away from zones of compression (tectonic escape), to minimize topographic relief and to avoid subduction of buoyant continental material (Bozkurt 2001).

It is still debated whether the westward motion is driven by push forces caused by topography in eastern Turkey, or by pull forces caused by subduction south of the Aegean (see section on western Turkey) (Bozkurt 2001).

On the regional scale Şengör *et al.* (1985) initially identified four distinct Neotectonic provinces generated by the Neotectonic regime: (i) E Anatolian contractional province with N-S shortening; (ii) N Turkish province with E-W shortening; (iii) W Anatolian extensional province with N-S extension and (iv) Central Anatolian "ova" province with NE-SW shortening and NW-SE extension. The best example for such a relationship is observed in the East Anatolian Volcanic Province (Göncüoğlu 2019).

The Central Anatolian "ova" province with NE-SW shortening and NW-SE extension is another area of extensive volcanism (Central Anatolian Volcanic Province; Toprak and Göncüoğlu 1993b) during the Neotectonic period. The formation of auxiliary strike-slip faults and fault-zones (Ecemiş and Tuz Gölü faults, Dirik and Göncüoğlu 1996; Özsayın *et al.* 2013) in Central

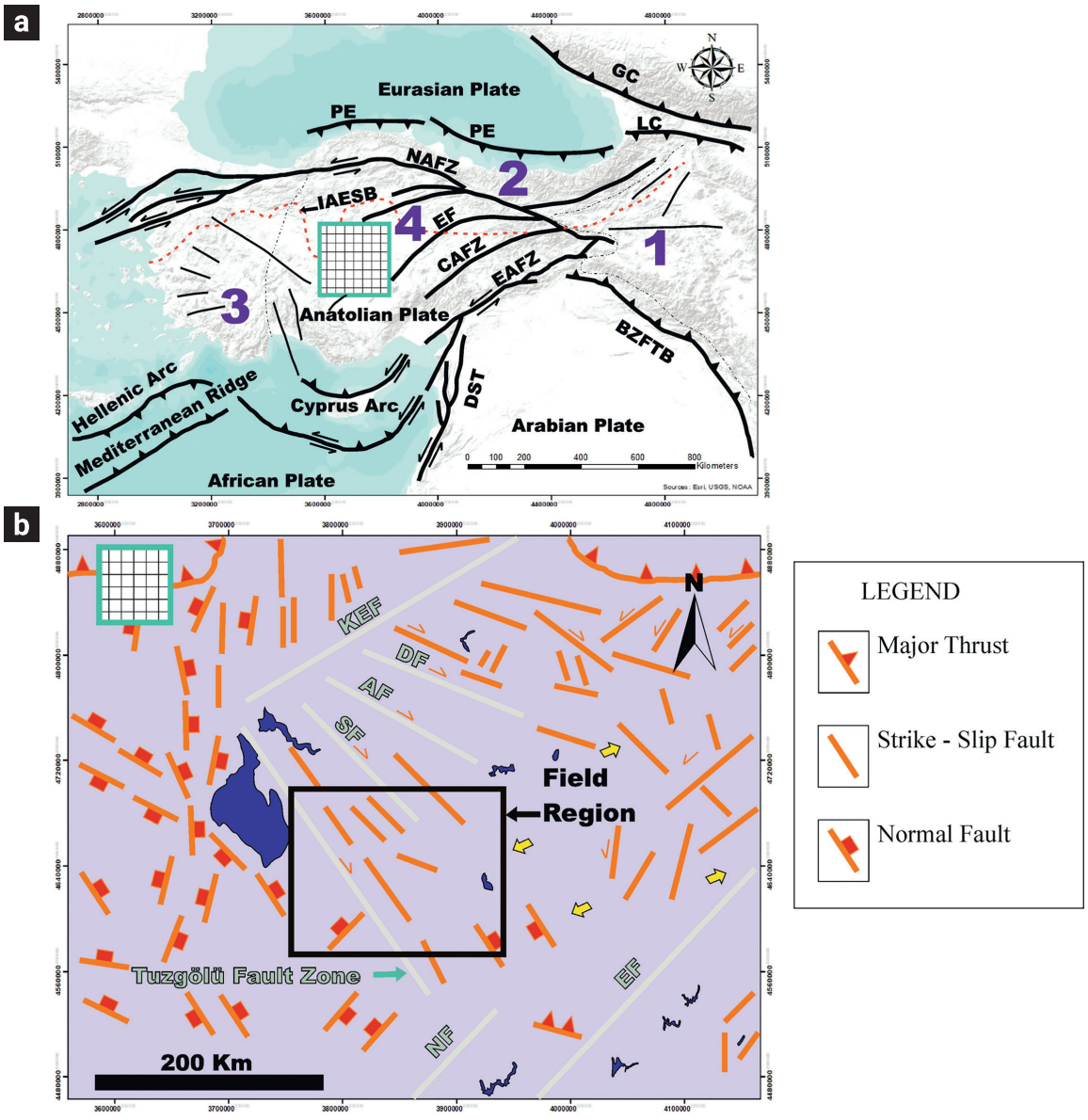

Figure 7. (a) Simplified tectonic map of Turkey (Explanations; 1: Anatolian Contractional Province, 2: North Anatolian Province, 3: West Anatolian Extensional Province, 4: Central Anatolian "OVA" Province, IAESB: Izmir – Ankara – Erzincan Suture Belt, BZFTB: Bitlis – Zagros Fold and Thurst Belt, NAFZ: North Anatolian Fault Zone, EAFZ: East Anatolian Fault Zone, CAFZ: Central Anatolian Fault Zone, DST: Dead Sea Transform, EF: Ecemiş Fault, PE: Pontic Escaipment, LC: Lesser Caucasus, GC: Greater Caucasus (b) Simplified neotectonic map of Tuzgölü and its vicinity (Explanations; KEF: Kirikkale – Erbaa Fault, SF: Salanda Fault, AF: Akpınar Fault, DF: Delice Fault, EF: Ecemiş Fault, NF: Niğde Fault) (Dirik and Göncüoğlu, 1996; Bozkurt 2001; Göncüoğlu 2019)

Anatolia along which Late Neogene–Quaternary pull-apart basins were generated.

Important volcanic centres such as Erciyes, Melendiz and Hasandag stratovolcanoes were formed on the intersection of the main strands of these faults (Toprak and Göncüoğlu 1993b). The Neogene-Quaternary volcanism in central Anatolia is mainly characterised (Kuscu-Gençalioğlu and Geneli 2010) by calc-alkaline andesites-dacites, with subordinate tholeiitic-mildly alkaline basaltic volcanism of the monogenetic cones.

Active tectonics of Turkey is the manifestation of collisional intracontinental convergence- and tectonic escape-related deformation since the Early Pliocene (~5 Ma). Three major structures govern the neotectonics of Turkey; they are dextral North Anatolian Fault Zone (NAFZ), sinistral East Anatolian Fault Zone (EAFZ) and the egean-cyprean Arc (Bozkurt 2001).

The present configuration of the NAFZ master strand and its splays form a typical fishbone structure (Şengör and Barka 1992;

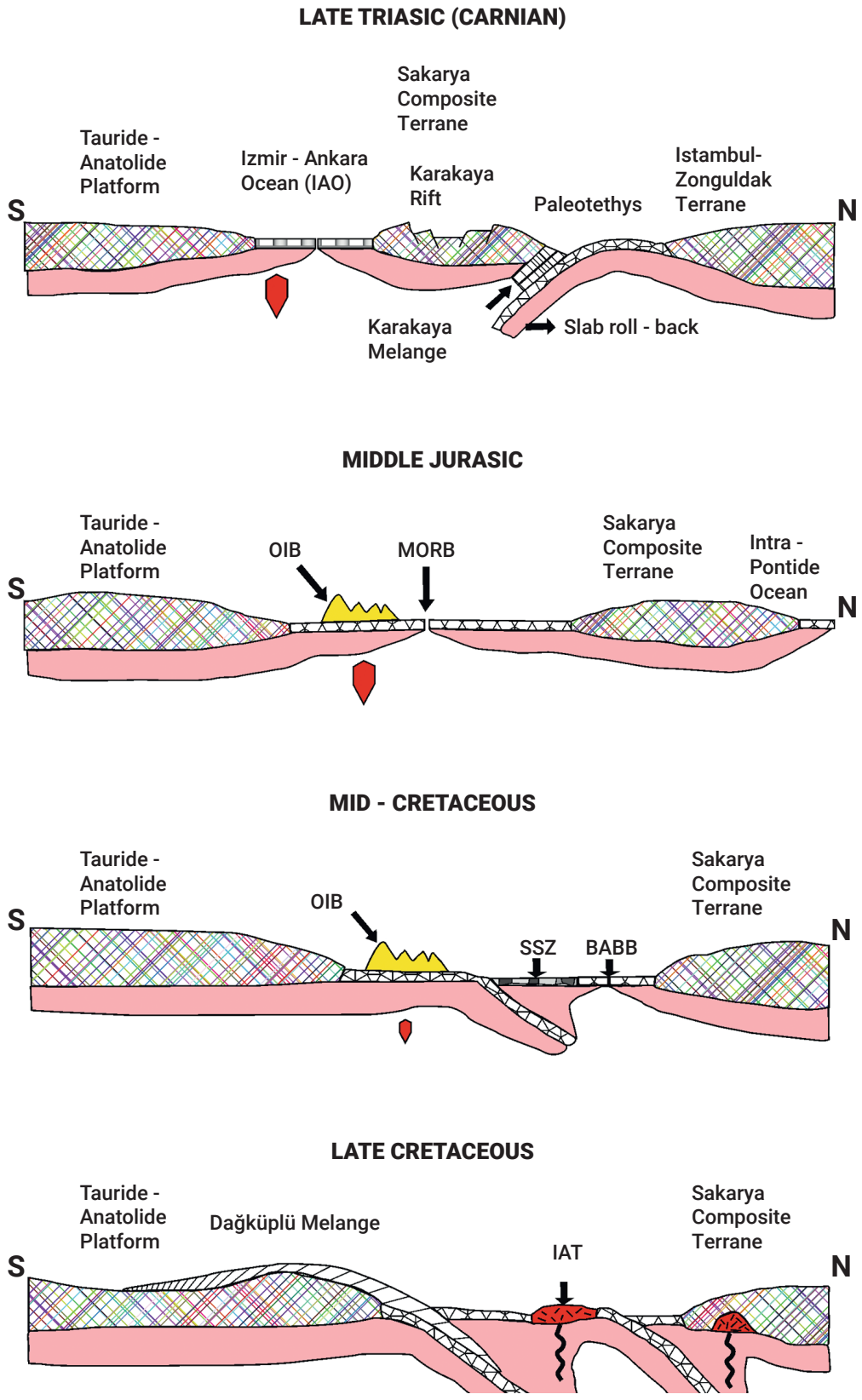

Figure 8. Geodynamic scenario depicting the geological evolution of the Izmir-Ankara-Erzincan Suture Belt. (Göncüoğlu 2019) (Explanations: OIB: Ocean Island Basalt, MORB: Mid – Ocean Ridge Basalts, SSZ: Suprasubduction Zone).

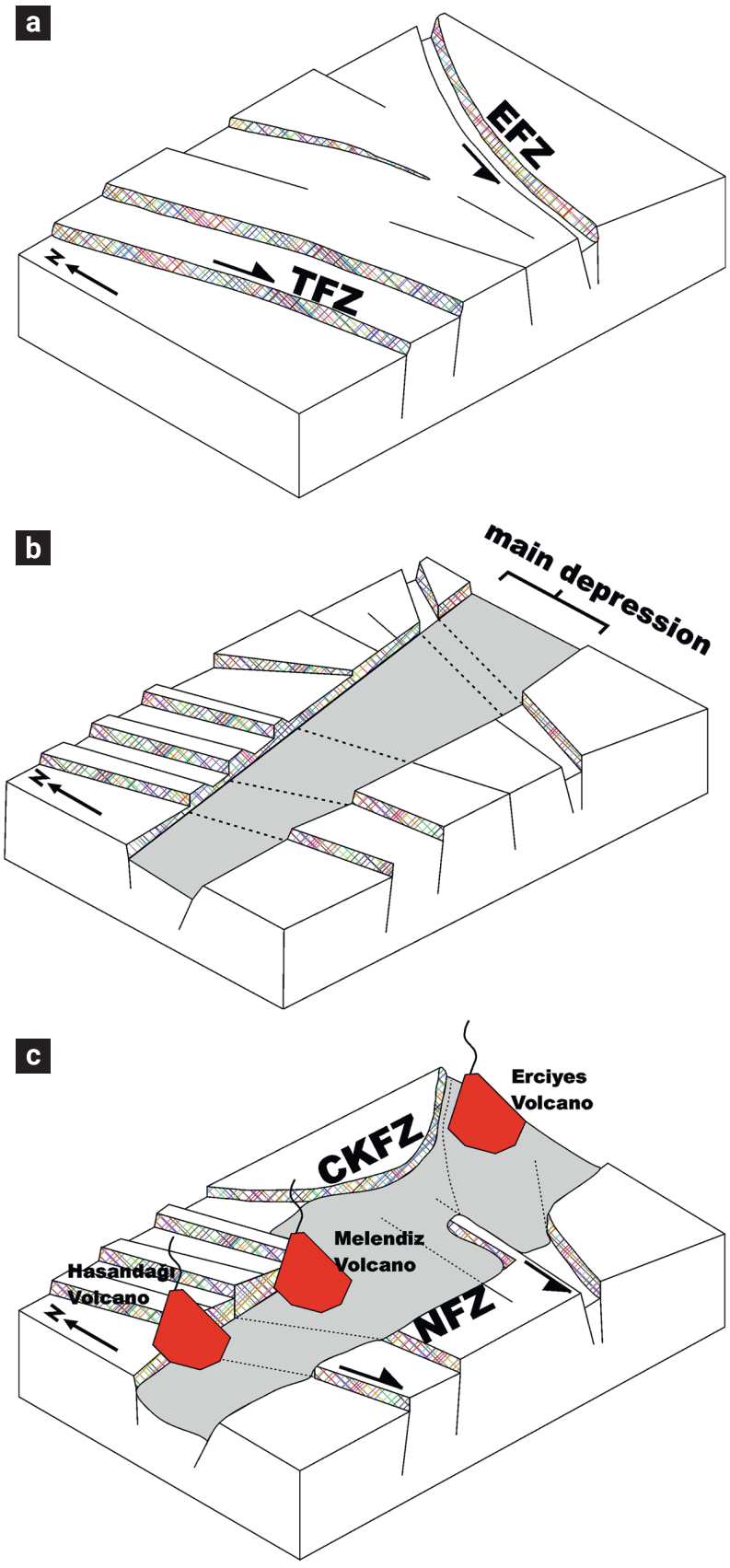

Figure 9. Relationship between active tectonics and volcanism in the Central Anatolian Volcanic Province and surrounding areas (Toprak and Göncüoğlu 1993b; Toprak 1998; Göncüoğlu 2019). (a) Pre-Mid Miocene, (b) Mid Miocene-Early Pliocene, (c) Late PlioceneQuaternary. (Explanations: TFZ Tuzgölü Fault Zone, EFZ Ecemiş Fault Zone, NFZ Niğde Fault Zone, CKFZ Central Kızılırmak Fault Zone).

Bozkurt 2001), which is created by the rotation of 'en echelon' wedges away from the main NAFZ.

They branch off the NAFZ and trend in approximately E-W direction for some distance. Then, they bend southwards and trend in an approximately NE to NNE-direction running into the Anatolian Plate.

The Central Anatolian Fault Zone (CAFZ) is a 730 km long sinistral mega shear zone, formed by the reactivation and propagation of an older palaeotectonic structure, namely the 'Ecemiş Corridor' or 'Ecemiş Fault' in the Plio-Quaternary times as a result of continued intracontinental convergence between the Arabian and Eurasian plates (Koçyigit and Beyhan 1998).

The fault zone runs from Erzincan in the northeast to the Eastern Mediterranean Sea (Figure 7a). It is seismically less active and comprises numerous segments. Total displacements during the palaeotectonic and neotectonic periods are 75 km and 24 km, respectively.

It is speculated that although the present-day slip along the CAFZ is only 3 mm/yr this system form the eastern boundary of the Anatolian Plate instead of the East Anatolian Fault Zone in the future (Koçyigit and Beyhan 1998).

The Central Anatolian Wedge (Figure 7a) is a region where discrete pieces of continental lithosphere deformed internally and produced a large bulk strain that thus has resulted in the generation of new structures or reactivation of old structures.

Some important strike-slip faults have been identified in Central Anatolia; Delice fault, Akpınar fault, Salanda fault, Ecemiş fault, Niğde fault and Tuzgölü fault zone.

The Tuzgöllü Fault Zone (TFZ) (Arpat and Şaroğlu 1975; Şengör *et al.* 1985), a 200-km-long, northwest-trending dextral strike-slip fault zone, is one of the most prominent structures of Central Anatolia (Figure 7b). The fault zone bounds the northeastern margin of the Tuzgöllü basin.

The initiation of movement along the TFZ is Late Cretaceous (Görür *et al.* 1984; Çemen *et al.* 1999), but there are also claims that the fault zone became active during the Miocene (Dellaloğlu and Aksu 1984). The fault zone is a strike-slip fault with a considerable normal component. The N-S and NE-SW trending distribution of volcanic cones is attribu ted to the dextral and normal faulting along the Tuzgöllü Fault Zone.

The historical and instrumental earthquake records show that the eastern parts of Central Anatolia is seismically less active, when compared with other parts of Anatolia The region has experienced a number of historical and instrumental earthquakes, such as the 1717 and 1835 Ecemiş. May 1914 Gemerek (M = 5.6), 1938 Kırşehir (M = 6.8), 2 1 February 1940 Erciyes (M = 5.3), and 14 August 1996 Mecitözü- Çorum (M = 5.6) earthquakes, which occurred along this structure.

In contrast to its eastern parts, the western parts of the Central Anatolia is dominated by a series of NE- SW- and NW- SE trending cross-graben and horst structures bounded by active, oblique-slip normal faults with strike-slip components (Figure 7a,b) (Bozkurt 2001).

6. Geothermal System Model

Geothermal systems have a very complex structure and consist of a heat source, an aquifer that can hold large amounts of water and steam, a capping rock that prevents heat and steam loss, and a recharge source that provides water to the aquifer. A modeling approach should be used to predict changes depending on the nutrition-excretion relationship in a complex system.

The heat source of the hydrothermal system in the Yaprakhisar Ziga geothermal area is probably volcanic activity. In the 2-dimensional (2-D) magnetotelluric modeling created according to the results of the magnetotelluric (MT) study conducted in the region, A low-resistivity mass (7-24 Ohm m) located at a depth of approximately 8 km within the crust with high resistance reaching 1000 Ohm m has been intruded into the crust, partially molten or solid but has not lost its temperature yet, and is interpreted as magmatic intrusion, which is thought to constitute the heat source of the geothermal system (Burçak 2006; TUBİTAK 2019).

The cap rock of the system is impermeable Upper Miocene-Pliocene-aged ignimbrite tuff and sediments formed in continental and lacustrine facies of the same age. It is thought shallow reservoirs developed in the permeable zones within these units.

The reservoir rocks of the system are permeable. In the MT model, the high resistivity (16 - 67 Ohm m) unit underneath the low resistivity unit interpreted as a cap rock was determined as a deep reservoir (500 - 1,500 m) formed by Paleozoic aged marble schists and gneisses (Burçak 2006; TUBİTAK 2019) (Figure 10).

In the study by Ölmez and Gevrek (1991), the geothermal gradient was determined as 0.62 °C / 10 m in the Ziga-1 well and 0.53 °C / 10 m in the Ziga-2 well. These values are nearly twice the average geothermal gradient (Burçak 2006; TUBİTAK 2019).

7. Field Applications

This study aims to investigate the shallow circulation geothermal potential in Selime and its surroundings. For this reason, vertical electric sounding (VES) profiles were made on the Selime tuff (Türker at al. 1991). Thermal fluid outflows were observed around the study area. However, these thermal outputs often mix with meteoric waters and surface waters. For this reason, the electrical resistivity method was used in the study to determine the thermal reservoir. As is known, the resistivity

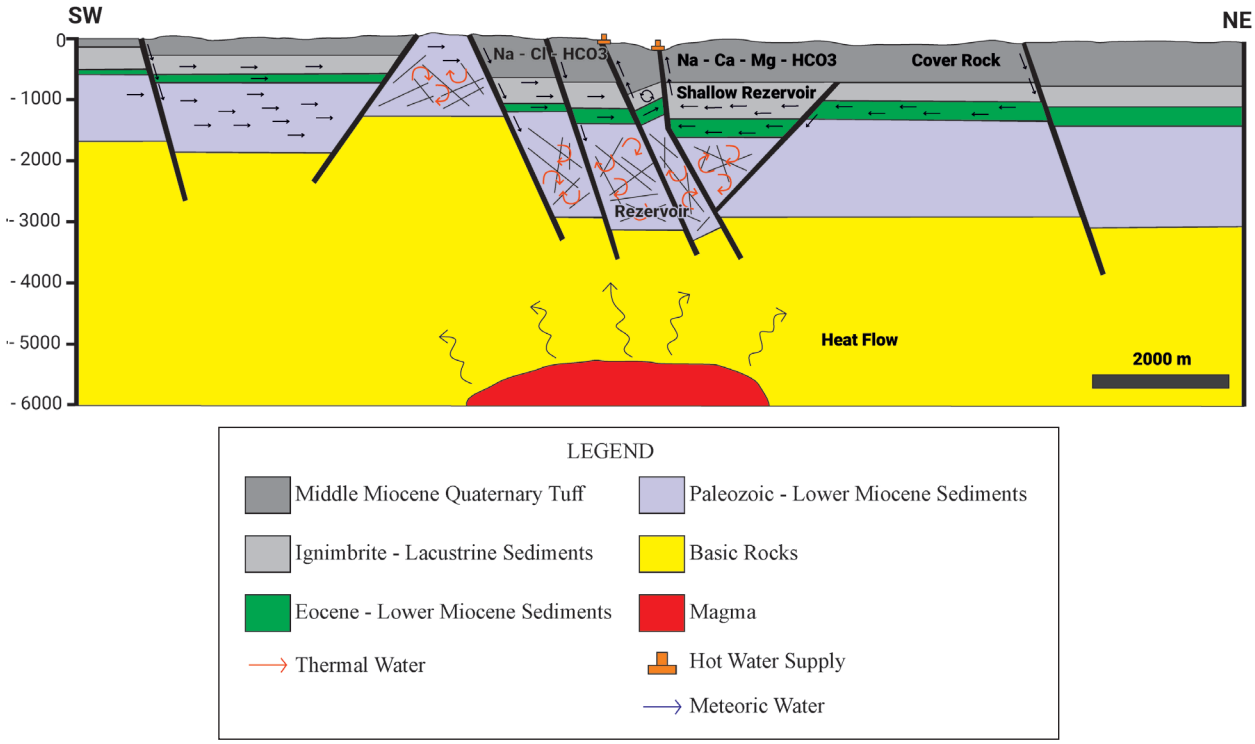

Figure 10. Circulating Geothermal Model (Burçak, 2006).

method, in general, is to measure the potential distribution of the electric field created in the ground. Indeed, the effect of shallow thermal circulation is characterized by the sudden peak drop in the resistivity curve. With this sudden increase in conductivity, the potential difference values in the receiver unit are also low.

Therefore, the potential difference being close to zero is by the general Ohm's law. To minimize the error rate, the configuration geometry was changed by increasing the MN intervals 5 vertical electrical soundings were made at the determined vertical electrical points (Figure 4b). A total of two A-profiles and three B-profiles in the were measured. The full Schlumberger configuration with four electrodes was used for the measurements. According to the applied electrode array, the maximum depth is AB/2 = 300m. Along this depth, it is important to determine the layer boundaries depending on the relationship between the thickness (m) and resistivity (ρ) of the layers (Figure 4b).

8. Geophysical Research and Resistivity, Magnetic, Gravity Methods

Hydrogeophysical research establishes a correlation between them using appropriate geophysical methods, especially in determining the thermal system. Gravity, magnetic and electrical (resistivity) methods are generally used in potential geothermal field exploration. For these methods, differences in physical parameters such as magnetic permeability and resistivity arising from the thermal fluid are essential. In addition, heat flux Q (cal/cm^{2}sec) data and chemical analyses contribute significantly to the determination of geothermal fields.

Geothermal systems are formed when meteoric waters circulate within the earth's crust, collecting the earth's internal heat or ground heat at high temperatures. For this reason, a geothermal circulation system ensures that meteoric waters are heated over a wide area on a regional scale and that the crust is heated by gravity and convection in high-temperature permeable environments.

However, the necessary conditions must be met to form a geothermal resource known to be of meteoric origin (İlkişik 1997; Koşaroğlu *et al.* 2016; Çetin *et al.* 2020). These conditions: First, a heating source is required. Therefore, meteoric nutrition must be maintained in the geothermal system. Geological layers such as an impermeable base rock, a permeable geothermal reservoir layer, and a fine-grained impermeable cover layer should be formed on top. Regional heat collection and circulation areas should be in horizontal and vertical directions.

The findings obtained in the vertical electrical drilling (VES) study conducted in the Selime geothermal field are compatible with the gravity and magnetic data in the field. Accordingly, the general criteria indicating the existence of a geothermal field must

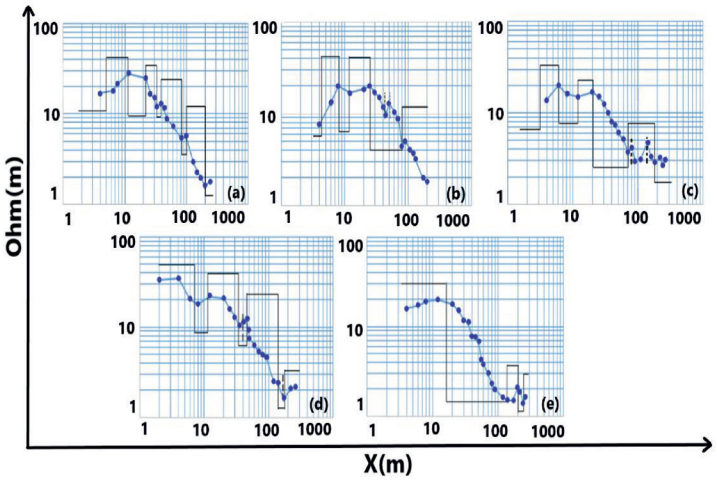

Figure 11. (a) A1 Profile. Depth(m), (b) A2 Profile. Depth(m),(c) B1 Profile. Depth(m),(d) B2 Profile. Depth(m), (e) B3 Profile. Depth(m) - Resistivity (Ohm-m) relationship.

be compatible and verified by the applied geophysical methods. These findings are correlated with resistivity-based studies and gravity and magnetic applications in the Selime thermal area, and the results are listed below.

8.1. Resistivity Method

Generally, the resistivity values of fluids in geothermal areas are low. As vertical electrical drilling increases towards depth, resistivity values decrease depending on the temperature. The resistivity profiles in the study confirmed this situation (Figure 11).

Hydrothermal alterations can be seen in volcanic fields. For this reason, in-field measurements show a sharp and sudden decrease in the resistivity values of the reservoir rock under the impermeable cover rock. Hydrothermal alterations have been observed in geological observations in the Selime research and surrounding areas. In addition, the presence of thermal fluid in the cracks and cracks of travertines also causes a decrease in resistivity.

8.2. Gravity Method

In gravity studies, the structural state of the field and the central tectonic units, such as the horst-graben and the basin of the field, are determined. In addition, identifying gravity-covered faults and fractures makes an essential contribution to geothermal fluid and thermal circulation (Figure 12).

Gravity evaluation was made according to the map with an average 2.4 g/cm^3 density. Frequency in gradients indicates possible faulting. For more detailed observation in the Ziga thermal area in the same thermal system as the Selime and Yaprakhisar areas, measurement intervals are 50 m. It has been determined that there are alteration zones between negative and positive inclusions in the gravity anomaly. In addition, the significant gradient in the Ziga, Selime, and Yaprakhisar areas indicates secondary faulting. Positive elevations in the Ziga thermal area are interpreted as foundation elevation (Akdoğan 1989).

8.3. Magnetic Method

This gas coming to the surface from the reservoir transforms the magnetite in the sedimentary or volcanic rocks, which it passes through into pyrite and thus affects the magnetic permeability of the rock. This change of geothermal origin is determined by the magnetic prospecting method. Selime in the field study: The resistivity study was correlated with the magnetic anomaly data 1988 by the Mineral Research and Exploration of Turkey (MTA), Geophysical Surveys Department. According to this, The high magnetic permeability zone on the Total Magnetic Anomaly map (Figure 13) has been confirmed to be a thermal area in Selime and Yaprakhisar and its surroundings. As a result, the field's deficient resistivity response was compatible with the gravity and magnetic data obtained in the region (Figure12 – Figure13).

9. Results

The SELIME region is a tourism region where tuff and fairy chimneys are located 5 km northwest of the Ihlara Valley, which is located in the world-famous Cappadocia complex region (Figure 2 – Figure 4a,b). Due to the significant decrease in the resistivity of the thermal underground waters in the rocks at high temperatures and the presence of mineral content in the thermal waters due to geothermal activity, geoelectric methods in geo-

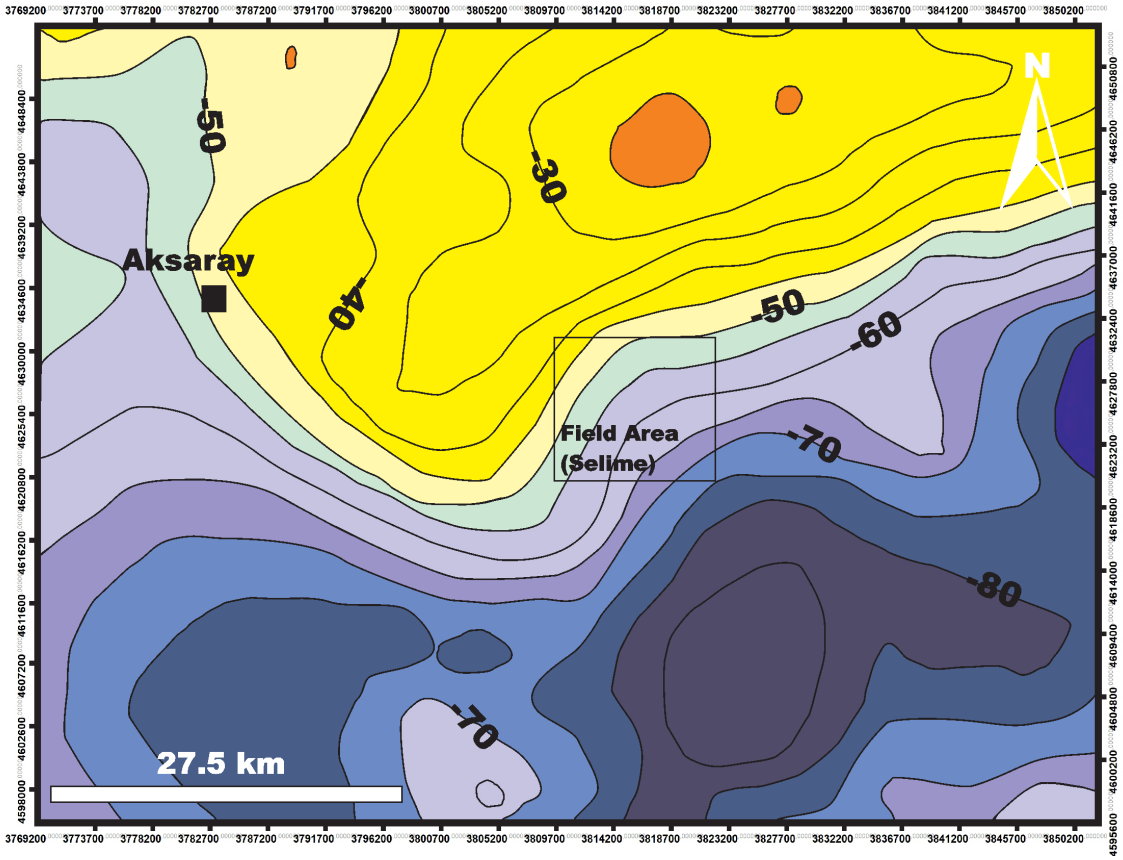

Figure 12. 2D Gravity anomaly in Selime and its vicinity. (Contour interval: 5 mGal).

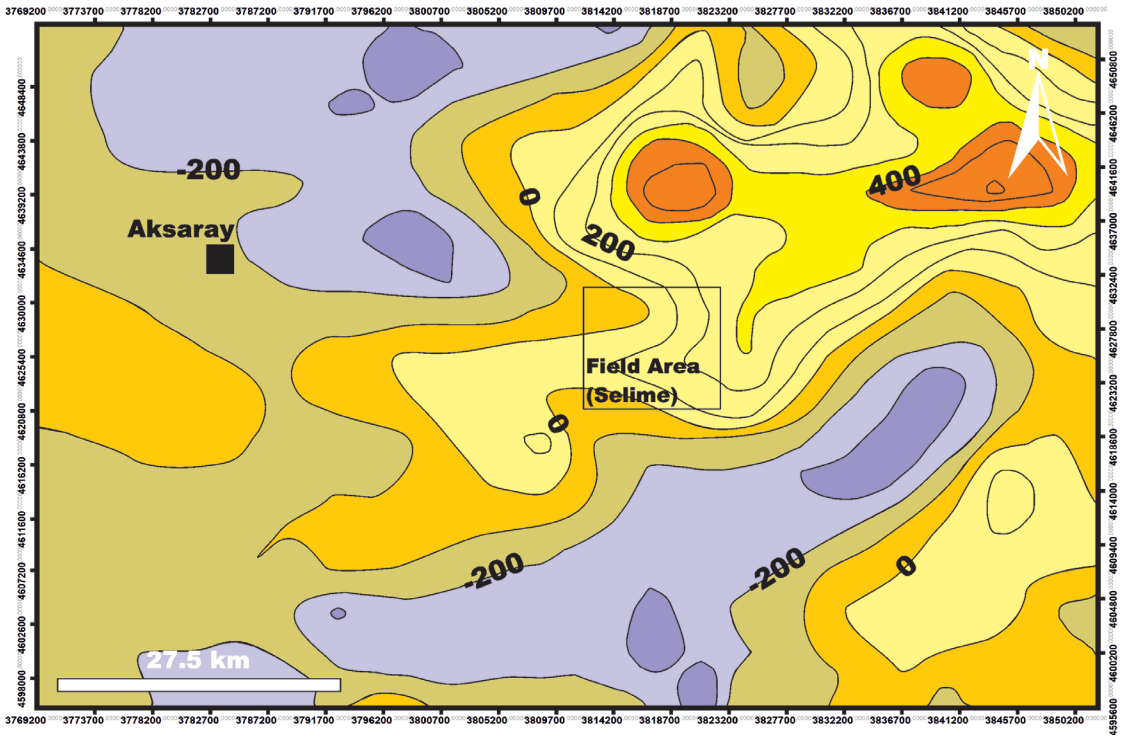

Figure 13. 2D Magnetic anomaly in Selime and its vicinity. (Contour interval: 100 nT).

thermal exploration have led to geothermal methods. Although it is known that conductivity increases with temperature, thermal fluid concentrated with salt ions also has good electrolytic conductivity. Five vertical electric Sounding (VES) has been carried out in the region. Schlumberger array geometry was used in the application, and the profile length is maximum AB/2=300 m.

According to the electrical resistivity studies carried out in the field, in the A1 VES (Vertical Electrical Sounding) profile (Figure 11), There is a 7 m thick and 13 Ohm-m resistive clay-containing Nojen vegetative cover layer. Under this layer, 28 m thick Selime tuff with 60 Ohm-m resistivity was located. The resistivity of the unit under this tuff showed a sudden decrease around 1-2 Ohm-m. In a similar situation, the A2 VES profile (Figure 11b) is also tuff-transitive but has identical values (Figure 11).

B1-B2-B3 VES profiles are similar (Figure 11c, 11d, 11e). Under the average 7-8 m and 11 Ohm-m vegetative layer, the 34 m thick Selime tuff with 52 Ohm-m resistivity is located. The resistivity of the unit under this tuff was observed to be around 1-2 Ohm-m. All three VES profiles are in similar condition, and a fractured structure has been determined, although they have a low resistivity medium (Figure 11c, 11d, 11e). When both measurement profile groups are examined, resistivity values fall sharply. Physically, there are two reasons for this: the density of the salt ions and the temperature. However, this area, which we discussed as a shallow circulation of Selime tuff, was determined to be an ideal impermeable cover rock.

According to the studies and other geophysical applications in the region, the following results were obtained:

1. Active faulting and fracture systems of the region developed under the control of the Tuz Gölü Fault Zone (Figure 4a - Figure 7b - Figure 10). The thermal fluid in this zone continues with shallow and deep circulation.
2. The impermeable Selime tuff is an ideal cover rock for the Selime geothermal potential system.
3. As a result of hydrogeological studies and electrical resistivity application in the field, broken zones were determined in the upper parts of the reservoir rock.
4. Together with the applied geophysical measurement data, impermeable tuff, and fracture systems, thermal outflows and travertine formations around Selime indicate the existence of a shallow circulation geothermal model in the research area.

10. Discussion

In 1988 and 1990, geoelectromagnetic surveys were undertaken by Mineral Research and Exploration of Turkey (MTA) to confirm the presence of a relatively shallow (= 0.5-I km), hydrothermally caused conductive layer or zone. The Ziga geothermal area, which is close to the study area, has been identified, and today it is operated as a ziga geothermal hot water thermal hotel (Figure 2 – Figure 4a). Metin Ilkışık *et al.* detected five thermal hot water points in 1997 in the Ihlara Valley, which is 5 km to the southeast of the study area, and determined the temperature of the thermal water sources here to be between 24 and 51 °C.

The geothermal fields identified in Turkey are generally far from the city centers. The geothermal potential detected in the Selime region; is thought to be related to the geothermal areas in the Ihlara Valley and the Ziga region geothermal fields, which were determined in previous studies. Where does the last link of this chain-linked relationship end? And how close is the last ring to Aksaray city center? The closer a detected geothermal resource is to big city centers, the more likely that geothermal resources can be used in heating and energy areas. Countries dependent on foreign natural gas, such as Turkey, should use their geothermal resources in heating and energy fields, which are more important than tourism.

This modest study conducted in the Selime region showed that the Ihlara Valley and the Ziga geothermal field line continued in the northwest direction and revealed that the interrelated geothermal areas were a little closer to the Aksaray city center.

11. Conflict of Interests

The authors declare that they have no conflict of interest for Investigation of the geothermal system in region of Selime (Turkey) by resistivity methods.

12. Data availability

Data will be made available on request.

13. Acknowledgments

We would also like to thank all our referees who self-criticized our article and made positive suggestions.

14. References

Akdoğan, N. (1989). *Aksaray (Nigde) Ihlara Vadisi jeotermal enerji aramaları gravite etüdü Raporu: MTA Genel Müdürlüğü.* (Report No. 10040). Ankara.

American Geology Institute. (2009). *American Geology Institute (AGI)*. **https://www.americangeosciences.org/about**

Arpat, E., & Şaroglu, F. (1975). Türkiye'deki bazı önemli genç tektonik olaylar, *Bulletin Geology Social. Turkey* 18, 91-101.

Asfahani, J. (2021). New semı-quantıtatıve approach for ınterpretıng vertıcal electrıcal soundıng (ves) measurements – usıng a fractal modelıng technıque, case study from khanasser valley, northern syrıa. *Geofísica Internacional*, 60(3), 211-228. doi: **https://doi.org/10.22201/igeof.00167169p.2021.60.3.1920**

Ateş, A., Bilim, F., & Buyuksarac, A. (2005). Curie Point Depth Investigation of Central Anatolia, Turkey. *Pure and Applied Geophysics*, 162(2), 357–371. doi: **https://doi.org/10.1007/s00024-004-2605-3**

Aydemir, A. (2009). Tectonic investigation of Central Anatolia, Turkey, using geophysical data. *Journal of Applied Geophysics*, 68,321-334. doi: **https://doi.org/10.1016/j.jappgeo.2009.02.002**

Aydemir, A., Bilim, F., Kosaroglu, S., & Buyuksarac, A. (2019). Thermal structure of the Cappadocia region, Turkey: a review with geophysical methods. *Mediterranean Geoscience Reviews*, 1,243-254. doi: **https://doi.org/10.1007/s42990-019-00011-7**

Ayhan, A.K., & Papak, I. (1988). *Aksaray-Taspinar-Altınhisar-Ciftlik-Delihebil (Nigde) civarinin jeolojisi.* (MTA Report No. 8315).

Başel, E.D.K., Serpen, Ü., & Satman, A., (2010). Turkey geothermal resource assessment. *Proceedings World Geothermal Congress, Bali, Indonesia*, 1–7.

Başokur, A. T., Koçyigit, A., Hacıoglu, O., Arslan, H.I., & Meqbel, N. (2022). Magnetotelluric imaging of the shallow-seated magma reservoir beneath the Karadag ˘ stratovolcano, Central Anatolia, Turkey. *Journal of Volcanology and Geothermal Research*, 427,107567. doi: **https://doi.org/10.1016/j.jvolgeores.2022.107567**

Bayrak, M., Serpen, Ü., & Ilkişik, O.M. (2011). Two-dimensional resistivity imaging in the Kızıldere geothermal field by MT and DC methods. *Journal of volcanology and geothermal research* 204(1), 1-11. doi: **https://doi.org/10.1016/j.jvolgeores.2011.05.005**

Beekman, P.H. (1966). *Geology Report of Aksaray Gelveri Çınarlı Area (north of Hasandağ Melendiz Mountain range)*. MTA Institute Geology Department, Turkey.

Benli, H. (2013). Potential of renewable energy in electrical energy production and sustainable energy development of Turkey: Performance and policies. *Renewable Energy*. 50, 33-46. doi: **https://doi.org/10.1016/j.renene.2012.06.051**

Berktold, A. (1983). Electromagnetic studies in geothermal regions. *Geophysical Surveys*, 6, 173-200. doi: **https://doi.org/10.1007/BF01454000**

Besang, C., Eckhardt, F.J., Harre, W., Kreuzer, H., & Müller, P. (1977). Radiometrische Altersbestimmungen an Neogenen Eruptivgsteinen der Türkei. *Geologisches Jahrbuch, Reihe B*, 25, 3–36.

Bozkurt, E. (2001). Neotectonics of Turkey–a synthesis. *Geodinamica Acta*, 14(1-3), 3-30. doi: **https://doi.org/10.1080/09853111.2001.11432432**

Burçak, M. (2006). *Aksaray jeotermal sahaları (Acıgöl, Ziga, Şahinkalesi) jeotermal ısı kaynaklarının araştırılması ve jeotermal sistemlerin kavramsal modellenmesi, orta Anadolu Türkiye.* [Master's Thesis]. Department of geological engineering, faculty of engineering, Niğde University.

Cortes, A.,R.,P., Moreira, C., A., Veloso, D., I., K., Vieira, L., B., & Bergonzoni, F. A. (2016). Geoelectrical prospecting for a copper-sulfide mineralization in the Camaquã sedimentary basin, Southern Brazil. *Geofísica Internacional*, 55-3, 165-174. doi: **https://doi.org/10.19155/rgi20165531608**

Cumming, W. (2009). *Geothermal resource conceptual models using surface exploration data.* [Proceeding]. 34th Workshop on Geothermal Reservoir Engineering.

Çemen, İ., Goncüoğlu, M.C., & Dirik, K. (1999). Structural evolution of the Tuzgolü basin in Central Anatolia, Turkey. *The Journal of Geology*, 107(6), 693-706. doi: **https://doi.org/10.1086/314379**

Çetin, A., Kadioglu, K.Y., & Paksoy, H. (2020). Underground thermal heat storage and ground source heat pump activities in Turkey. *Solar Energy*, 200, 22-28. doi: **https://doi.org/10.1016/j.solener.2018.12.055**

Çiner, A., Dogan, U., Yıldırım, C., Akçar, N., Ivy-Ochs, S., Alfimov, V., Kubik, P.W., & Schlüchter, C. (2015). Quaternary uplift rates of the Central Anatolian Plateau, Turkey: insights from cosmogenic isochron-burial nuclide dating of the Kızılırmak River terraces. *Quaternary Science Reviews*, 107, 81–97. doi: **https://doi.org/0.1016/j.quascirev.2014.10.007**

Dellaloğlu, A.·&·Aksu R., (1984). *Kulu-Şereflikoçhisar Aksaray Dolayının Jeolijisi ve Petrol Olanaklan, Turkish Petroleum Corporation.* (Report No. 2020).

Dentith, M., & Mudge, S.T. (2014). Geophysics for the mineral exploration geoscientist. *Cambridge University Press, Cambridge*, 50(1), 1-2. doi: **https://doi.org/10.1007/s00126-014-0557-9**

Dirik, K., & Göncüoğlu, M.C. (1996). Neotectonic characteristics of the Central Anatolia. *International Geology Review*, 38(9), 807-817. doi: **http://doi:10.1080/00206819709465363**

Flores, C., & López-Moya, A. (2011). A comparison of three geoelectric methods in the presence of shallow 2-D inhomogeneities: A case study. *Geofísica Internacional*, 50(4), 371-399. doi: **https://doi.org/10.22201/igeof.00167169p.2011.50.4.151**

Froger, J.L., Lenat, J.F., Chrowicz, J., Le Pennec, J.L., Bourdier, J.L., & Kose, O. (1998). Hidden calderas evidenced by multisource geophysical data; example of Cappadocian Calderas. *Journal of Volcanology and Geothermal Research*, 85(1-4), 99-128. doi: **https://doi.org/10.1016/S0377-0273(98)00052-3**

Gans, C.R., Beck, S.L., Zandt, G., Berk, C.B., & Özacar, A.A. (2009). Detecting the limit of slab break-off in central Turkey: new high-resolution Pn tomography results. *Geophysical Journal International*, 179(3), 1566-1572. doi: **https://doi.org/10.1111/j.1365-246X.2009.04389.x**

Giggenbach, W.F. (1988). Geothermal solid equilibrie. Derivation of Na-K-Mg-Ca geoindicators. *Geochemica at Cosmochimica Acta*, 52(12), 2749-2765. doi: **https://doi.org/10.1016/0016-7037(88)90143-3**

Gomez, R.C., Kereszturi, G., Whitehead, M., Reeves. R., Rae, A., & Pullanagari, R. (2023). Point pattern analysis of thermal anomalies in geothermal fields and its use for inferring shallow hydrological processes. *Geothermics*, 110, 102664. doi: **https://doi.org/10.1016/j.geothermics.2023.102664**

Göncüoğlu, M. C. (2019). A Review of the Geology and Geodynamic Evolution of Tectonic Terranes in Turkey. *Mineral Resources of Turkey*, 16,19–72. doi: **https://doi.org/10.1007/978-3-030-02950-0_2**

Göncüoğlu, M.C., Tekin, U.K., Sayit, K., Bedi, Y., & Uzunçimen, S. (2015). Opening, evolution and closure of the Neotethyan oceanic branches in Anatolia as inferred by radiolarian research. *Radiolaria*, 35,88–90.

Görür, N., Oktay, F.Y., Seymen, İ., & Şengör, A.M.C. (1984). Palaeotectonic evolution of Tuzgölü basin complex, Central Turkey. En A. Dixon J.E., Robertson A.H.F. (Eds.). *The geological evolution of the Eastern Mediterranean.* (pp. 81-96) Geological Society Spectal, London.

Gyulai, A., Szucs, P., Turai, E., Baracza, M.K., & Fejes, Z. (2016). Geoelectric ↑Characterization of Thermal Water Aquifers Using 2.5D Inversion of VES ↑Measurements. *Surveys in Geophysic*, 38, 503-526. doi: **https://doi.org/10.1007/s10712-016-9393-z**

Hacıoğlu, O., Başokur, A.T., Meqbel, N., Arslan, H.I., & Efeçinar, T. (2023). Magnetotellurics unveils a hidden caldera complex beneath the Cappadocia Volcanic Province, Central Anatolia, Türkiye. *Journal of Volcanology and Geothermal Research*, 442, 107877. doi: **https://doi.org/10.1016/j.jvolgeores.2023.107877**

Hedenquist, J. W., & Browne, P. R. L. (1989). The evolution of the Waiotapu geothermal system, New Zealand, based on the chemical and isotopic composition of its fluids, minerals and rocks. *Geochimica et Cosmochimica Acta*, 53(9), 2235–2257. doi: **https://doi.org/10.1016/0016-7037(89)90347-5**

Ilkişik, O.M., Gürer, A., Tokgöz, T., & Kaya, C. (1997). Geoelectromagnetic and geothermic investigations in the Ihlara Valley geothermal field. *Journal of Volcanology and Geothermal Research*, 78(3), 297-308. doi: **https://doi.org/10.1016/S0377-0273(97)00008-5**

Kaygusuz, A., Siebel, W., Şen, C., & Satir, M. (2008). Petrochemistry and petrology of I-type granitoids in an arc setting: the composite Torul pluton, Eastern Pontides, NE Turkey. *International Journal of Earth Sciences*, 97(4),739-764. doi: **http://dx.doi.org/10.1007/s00531-007-0188-9**

Keller G.V., & Frischknecht F.C. (1966). *Electrical methods in geophysical prospecting*. Pergamon Press.

Kıyak, A., Karavul, C., Gülen, L., Pekşen, E., & Kılıç, R.A. (2015). Assessment of geothermal energy potential by geophysical methods: Nevşehir Region, Central Anatolia. *Journal of Volcanology and Geothermal Research*, 295, 55–64. doi: **https://doi.org/10.1016/j.jvolgeores.2015.03.002**

Kirsch, R. (2006). *Grounwater geophysics, a tool for Hydrogeology*. Springer. doi: **https://doi.org/10.1007/978-3-540-88405-7**

Koçyigit, A., & Beyhan, A. (1998). A new intracontinental transcurrent structure: the Central Anatolian Fault Zone, Turkey, *Tectonophysics*, 284, 317-336. doi: **https://doi.org/10.1016/S0040-1951(97)00176-5**

Koçyiğit, A., Yılmaz, A., Adamia, S., & Kuloshvili, S. (2001). Neotectonics of East Anatolian Plateau (Turkey) and Lesser Caucasus: implication for transition from thrusting to strike-slip faulting. *Geodinamica Acta*, 14(1-3), 177-195. doi: **http://dx.doi.org/10.1016/S0985-3111(00)01064-0**

Korkmaz, E.D., Serpen, U., & Satman, A. (2014). Geothermal boom in Turkey: Growth in identified capacities and potentials. *Renewable Energy*, 68, 314-325. doi: **https://doi.org/10.1016/j.renene.2014.01.044**

Koşaroğlu, S., Büyüksaraç, A., & Aydemir, A. (2016). Modeling of shallow structures in the Cappadocia region using gravity and aeromagnetic anomalies. *Journal of Asian Earth Sciences*, 124, 214-226. doi: **https://doi.org/10.1016/j.jseaes.2016.05.005**

Kuscu-Gençalioğlu, G., & Geneli, F. (2010). Review of post-collisional volcanism in the Centra Anatolian Volcanic Province (Turkey), with special reference to the Tepekoy Volcani Complex. *International Journal of Earth Sciences* 99(3), 593-621. doi: **https://doi.org/10.1007/s00531-008-0402-4**

Lloyd, E.F. (1959). The Hot Springs and Hydrothermal Eruptions of Waiotapu. New Zealand. *Journal of Geology and Geophysics*, 2(1), 141–176. doi: **https://doi.org/10.1080/00288306.1959.10431319**

Lowrie, W. (2007). Fundamentals of Geophysics. *Cambridge University Press*, New York. **https://doi.org/10.1017/S0016756808004871**

McNeill, J.D. (1990). Use of electromagnetic methods for groundwater studies. En A. Ward, S.H. (Ed.). *Geotechnical and environmenta geophysics* (pp. 191-218). Society of Exploration Geophysicists.

Meju, M.A. (2002). Geoelectromagnetic Exploration for Natural Resources Models, Case Studies and Challenges. *Surveys in Geophysics*, 23(2), 133-206. doi: **https://doi.org/10.1023/A:1015052419222**

Mineral Research and Exploration of Turkey (MTA) (1988). Department of Geophysical Studies, Geothermal Energy Searches, Aksaray-IHLARA Region, Turkey.

Montanaro, C., Ray, L., Cronin, S. J., Calibugan, A., Rott, S., Bardsley, C., & Scheu, B. (2023). Linking top and subsoil types, alteration and degassing processes at Rotokawa geothermal field, New Zealand. *Frontiers in Earth Science*, 10, 1067012. doi: **https://doi.org/10.3389/feart.2022.1067012**

Munoz, G. (2014). Exploring for geothermal resources with electromagnetic methods. *Surveys in Geophysics*, 35(1), 101–122. doi: **https://doi.org/10.1007/s10712-013-9236-0**

Öktü, G., & Kalkan, İ. (1984). *Niğde-Akaray Ziga Spa Hydrogeology Study*. (MTA Report No. 7505). Turkey.

Ölmez, E. & Gevrek, A.İ. (1991). *Aksaray-sofular 1 ve sofular 2 ile Ziga belisırma 1-2 gradyan sondajları kuyu bitirme raporu.* (MTA Report No. 9194, unpublished).

Özsayın, E., Çiner, A., Rojay, B., Dirik, K., Melnick, D., Fernandez-Blanco, D., Bertotti, G., Schildgen, T.F., Garcin, Y., & Strecker, M.R. (2013). Plio-Quaternary extensional tectonics of the Central Anatolian Plateau:

a case study from the Tuz Golü Basin, Turkey. *Turkish journal of earth sciences*, 22(5), 691-714. doi: **https://doi.org/10.3906/yer-1210-5**

Pasquare, G., Poli, S., Vezzoli, L., & Zanchi, A. (1988). Continental arc volcanism and tectonics setting in Central Anatolia, Turkey. *Tectonophysics*, 146, 217-230. doi: **https://doi.org/10.1016/0040-1951(88)90092-3.**

Pellerin, L., Johnston, J.M., & Hohmann, G.W. (1996). A numerical evaluation of electromagnetic methods in geothermal exploration. *Geophysics*, 61(1), 121-130. doi: **https://doi.org/10.1190/1.1443931**

Piper, J.D.A., Gürsoy, H., & Tatar, O. (2002). Palaeomagnetism and magnetic properties of the cappadocian ignimbrite succession, Central Turkey and Neogene tectonics of the Anatolian collage. *Journal of Volcanology and Geothermal Research*, 117(3), 237-262. doi: **https://doi.org/10.1016/S0377-0273(02)00221-4.**

Samrock, F., Kuvshinov, A., Bakker, J., Jackson, A., & Fisseha, S. (2015). 3-D analysis and interpretation of magnetotelluric data from the Aluto-Langano geothermal field, Ethiopia. *Geophysical Journal International*, 202(3), 1923–1948. doi: **https://doi.org/10.1093/gji/ggv270**

Sayit, K., Göncüoğlu, M.C., & Tekin, U.K. (2015). Middle Carnian arc-type basalts from the Lycian Nappes, Southwestern Anatolia: early late Triassic subduction in the Northern Branch of Neotethys. *The Journal of Geology*, 123(6),561-579. doi: **https://doi.org/10.1086/683664**

Serpen, U., & DiPippo, R. (2022). Turkey-A geothermal success story: A retrospective and prospective assessment. *Geothermics*, 101, 102370. doi: **https://doi.org/10.1016/j.geothermics.2022.102370**

Serpen, Ü., Aksoy, N., Öngür, T., & Korkmaz, E.D. (2009). Geothermal energy in Turkey:2008 update. *Geothermics*, 38, 227–237. doi: **https://doi.org/10.1016/j.geothermics.2009.01.002**

Şaroğlu, F., Emre, Ö., & Boray, A. (1992). *Türkiye Diri Fay Haritası, Active Faults maps of Turkey.* [Mapa]. 1:25000. MTA Publication, Ankara.

Şengör, A.M.C., & Barka, A.A. (1992). Evolution of escape-related Strike-slip systems: implications for distribution of collisional orogens. [Sesión de conferencia]. 29th International Geological Congress, Kyoto, Japan.

Şengör, A.M.C., Görür, N., & Şaroglu, F. (1985). Strike-slip faulting and related basin formation in zones of tectonic escape: Turkey as a case study. En A. Biddle K.T., Christie-Slick N. (Eds.), *Strike-slip Faulting and Basin Formation* (pp. 227-264) Soc. Econ. Paleontol. Mineral.

Tank, B.S., & Karaş, M. (2020). Unraveling the electrical conductivity structure to decipher the hydrothermal system beneath the Mt. Hasan composite volcano and its vicinity, SW Cappadocia, Turkey. *Journal of Volcanology and Geothermal Research*. 405, 107048. doi: **https://doi.org/10.1016/j.jvolgeores.2020.107048**

Tekin, U.K., Göncüoğlu, M.C., & Turhan, N. (2002). First evidence of late Carnian radiolarian fauna from the Izmir-Ankara Suture Complex, Central Sakarya, Turkey: implications for the opening age of the Izmir-Ankara branch of Neotethys. *Geobios*, 35(1), 127-135. doi: **https://doi.org/10.1016/S0016-6995(02)00015-3**

Toprak, V. (1998). Vent distribution and its relation to regional tectonics, Cappadocian Volcanics, Turkey. *Journal of Volcanology and Geothermal Research*, 85(1), 55–67. doi: **https://doi.org/10.1016/S0377-0273(98)00049-3**

Toprak, V., & Göncüoğlu, M.C. (1993b). Tectonic control on the development of the Neogene Quaternary Central Anatolian volcanic province. *Turkey Geology Journal*, 28, 357–369. doi: **https://doi.org/10.1002/gj.3350280314.**

TUBİTAK, (2019). *Geothermal resources evaluation project Aksaray Provincial Report. Turkish Scientific and Technical Research Council (TUBİTAK).*

Türker, A.E., Keçeli, D.A., Kaya, M.A., & Kamacı, Z. (1991). Uşak-Banaz Jeotermal Alanının Jeoelektrik Yöntemlerle Araştırılması. *Jeofizik*, 5, 59-74.

Ward, S.H. (1990). Resistivity and induced polarization methods. En A. Ward, S.H. (Ed.). *Geotechnical and environmental geophysics*. (pp. 147-189). Society of Exploration Geophysicists.